

Extreme fractionation from zircon to hafnon in the Koktokay No. 1 granitic pegmatite, Altai, northwestern China

RONG YIN¹, RU CHENG WANG^{1,*}, AI-CHENG ZHANG¹, HUAN HU¹, JIN CHU ZHU¹, CAN RAO² AND HUI ZHANG³

¹State Key Laboratory for Mineral Deposits Research, School of Earth Sciences and Engineering, Nanjing University, Nanjing 210093, China

²Department of Earth Sciences, Zhejiang University, Hangzhou 310027, China

³Institute of Geochemistry, Chinese Academy of Sciences, Guiyang, 550002, China

ABSTRACT

The Koktokay No. 1 pegmatite is a Li–Cs–Ta-rich granitic pegmatite located in Altai, northwestern China. Zircon is present in most textural zones of this pegmatite and in its contact zone with surrounding metagabbro. Here we describe the detailed associations of zircon with other minerals, and the internal textures and chemistry of the zircons. Most zircon grains from the contact zone have relatively low HfO₂ (<9.4 wt%), whereas the bright rim of one such grain has high HfO₂ (18.0–18.7 wt%). Zircon grains from the aplite zone contain <9.6 wt% HfO₂, although their thin and bright rims have higher HfO₂ (10.8–13.0 wt%). Most zircon grains from the quartz–muscovite zone have complex internal textures and have HfO₂ contents of <13.0 wt%. However, zircon grains from localized, nest-like, muscovite aggregates are highly enriched in HfO₂ (up to 36.1 wt%). Zircon (*sl*) from the cleavelandite–quartz–spodumene zone can be divided into two types based on petrography and chemistry. One group of zircons appears to be typical magmatic zircon and are greater than 100 μm in size, closely associated with albite, and have HfO₂ contents of 13.0–19.5 wt%. The second group of zircons is typically associated with muscovite and/or spodumene, is small in size (down to a few micrometers), and may exhibit zoning or alteration textures. The HfO₂ contents of this second zircon group are 19.8–58.9 wt%, indicating the presence of hafnian zircon to zirconian hafnon. Large HfO₂ content variations of up to 34.8 wt% were also observed within single zoned crystals. We suggest that the increase of HfO₂ in the magmatic zircon from 9.4 wt% in the contact zone to 19.5 wt% in the cleavelandite–quartz–spodumene zone mainly reflects fractional crystallization of pegmatite magma. However, the occurrence of hafnian zircon and hafnon in the cleavelandite–quartz–spodumene zone is likely related to coupled Li–F fluxing effects in the pegmatite magma.

Keywords: Zr–Hf fractionation, zircon, hafnon, granitic pegmatite, Altai

INTRODUCTION

Zirconium (Z = 40) and hafnium (Z = 72) are two neighboring elements in Group IVb of the Periodic Table and have similar ionic radii in most minerals (e.g., R_{Zr} = 0.84 and R_{Hf} = 0.83 Å at eightfold coordination; Shannon 1976). Consequently, Zr and Hf have similar crystal-chemical properties and constitute one of the most coherent element pairs in geochemical systems. Synthetic experimental results indicate that zircon (ZrSiO₄) and hafnon (HfSiO₄) constitute a complete solid solution (Ramakrishnan et al. 1969). Based on the Hf/[Zr + Hf] atomic ratio (Hf no.), the zircon–hafnon series can be divided into zircon (Hf no. = 0.0–0.1), hafnian zircon (Hf no. = 0.1–0.5), zirconian hafnon (Hf no. = 0.5–0.9), and hafnon (Hf no. = 0.9–1.0) (Correia Neves et al. 1974). Due to the similar chemical properties and almost identical ionic radii of Zr⁴⁺ and Hf⁴⁺, most magmatic processes cannot cause significant Hf enrichment in magmatic melts and zircons (Ellison and Hess 1986). In most types of rocks, HfO₂ contents in zircon are low (<3 wt% HfO₂; Belousova et al. 2002). The exception to this is some evolved granitic rocks

(Linnen and Cuney 2005), where zircon may have high HfO₂ with Hf no. values up to 0.35 (e.g., Wang et al. 1996; Zhang et al. 2004b; Ma and Rossman 2005; Van Lichtervelde et al. 2009). The Hf-dominant species such as zirconian hafnon and hafnon in the zircon–hafnon series have been reported in natural rocks, but are very rare, and have only been found in heavy mineral concentrates from their type locality (i.e., Ta-rich pegmatites in Zambézia, Mozambique; Correia Neves et al. 1974). Although the presence of these natural hafnon grains indicates that their host granitic pegmatites are highly evolved, the internal textures of the grains and their associations with other minerals have not been described (Correia Neves et al. 1974), which limits our understanding of the evolution from zircon to hafnon.

The Koktokay No. 1 pegmatite is a Li–Cs–Ta-rich (LCT-type) granitic pegmatite dike from the Chinese Altai in northwestern China. The zircon–hafnon series in this pegmatite has a strong zircon to hafnon evolution among different pegmatite zones and within single grains. HfO₂ contents in some zircon–hafnon grains are up to 58.9 wt% and correspond to a Hf no. value of 0.75 (zirconian hafnon). Herein, we describe the detailed mineralogical features of zircon–hafnon in this pegmatite and discuss the possible factors affecting the marked evolution from

* E-mail: rcwang@nju.edu.cn

zircon to hafnon within different pegmatite zones and single mineral grains.

GEOLOGICAL SETTING

The Chinese Altai pegmatite district is located in the southern part of the Altai orogenic belt, which extends from eastern Kazakhstan through Russia, northwestern China, and to southern Mongolia (Xiao et al. 1992; Windley et al. 2002). The world-renowned Altai pegmatite district comprises abundant pegmatite dikes over an area of ~20 000 km². Previous studies have identified ca. 100 000 pegmatite dikes in the Altai district (e.g., Wu and Zou 1989). The Koktokay No. 3 pegmatite is the largest dike of these highly evolved pegmatites, and is an economically important Ta-Be-Li-Cs deposit (Wang et al. 2007b). Rare element minerals in the Koktokay No. 3 pegmatite have been extensively studied (e.g., Wang et al. 1981; Zhang et al. 2004a, 2004b, 2008a, 2008b; Wang et al. 2006, 2007a, 2009). The Koktokay No. 1 pegmatite is located 1.2 km southwest of the No. 3 pegmatite at an altitude of ca. 1225–1430 m and was intruded into metagabbro (Fig. 1). The Koktokay No. 1 pegmatite is ~1400 m long, 1 to 7 m thick, and dips to the southwest at an average dip of 25°. The Koktokay No. 1 pegmatite was discovered in 1935 by a geological survey group from the former Soviet Union and has been exploited for beryl, spodumene, Nb-Ta oxides, and pollucite.

As part of the present study, detailed field investigations of the Koktokay No. 1 pegmatite were carried out at four prospects (Fig. 2a). The internal structure of the pegmatite is asymmetrical. Based on mineral assemblages, the following textural zones have been identified upward from the thin contact zone between the pegmatite and the surrounding metagabbro (Fig. 2b): an aplite zone (Zone I); a quartz–muscovite zone (Zone II); a cleavelandite–quartz–spodumene zone (Zone III); a blocky quartz zone (Zone IV); and a blocky microcline zone (Zone V).

The contact zone between the pegmatite and the surrounding metagabbro is several centimeters thick and is characterized by the presence of black, acicular crystals of schorl and apatite. Other minerals in the contact zone include quartz, holmquistite, kyanite, and manganocolumbite.

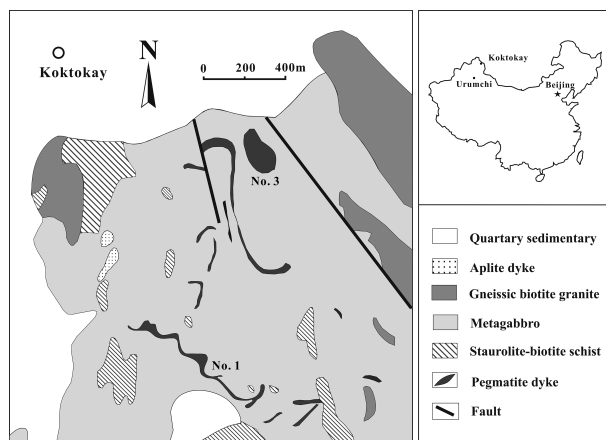


FIGURE 1. Geological map of the Koktokay pegmatite district of northwestern China (modified after Zhang et al. 2004b).

The aplite zone (Zone I) is ca. 2 m thick and comprises multiple white and gray layers (inset of Fig. 2a) of fine-grained albite (<100 μm in size) and quartz–muscovite (typically several hundred micrometers in size), respectively. Reddish and fine-grained spessartine is abundant in the dominant white layer and manganocolumbite is also present.

The quartz–muscovite zone (Zone II) varies in thickness from 0.5 to 2.0 m. This zone mainly comprises quartz and muscovite (usually >1 cm in size). Other common minerals include K-feldspar, albite, and beryl (up to 5 cm in size; inset of Fig. 2a). Locally, some nest-like muscovite aggregates up to several centimeters in diameter are present. The nest-like muscovite differs from other muscovite in this zone in two aspects. First, the nest-like muscovite is greenish in color, whereas the other muscovite in this zone is gray in color. Second, the nest-like muscovite is finer grained (<1 cm in diameter) than the other muscovite in this zone. Manganocolumbite is also present in this zone, but no spessartine was observed.

The cleavelandite–quartz–spodumene zone (Zone III) is present at prospects 2 and 3 and absent at prospects 1 and 4 (Fig. 2b). Zone III is up to 5 m thick in prospect 3. In addition to spodumene up to 2 m in length, this zone also contains other Li-rich minerals such as lepidolite and lithiophilite (inset of Fig. 2a). Columbite-group minerals are the dominant rare metal oxides and spessartine is also present.

The blocky quartz zone (Zone IV) is 1–3 m thick, although it was not observed in prospect 4. The blocky microcline zone (Zone V) is 1–3 m thick and is found in the uppermost part of the pegmatite.

ANALYTICAL METHODS

Petrographic textures of zircon–hafnon grains were observed under an optical microscope and by scanning electron microscopy at Nanjing University, Nanjing, China (JSM 6490), and at Purple Mountain Observatory, Nanjing, China (Hitachi 3400N II) using backscattered electron (BSE) imaging. Some BSE images were also obtained using a JEOL 8100 electron probe micro-analyzer (EPMA) at Nanjing University.

The mineral chemistry of zircon–hafnon was determined using the aforementioned EPMA equipped with four wavelength-dispersive spectrometers. The EPMA was operated at an accelerating voltage of 15 kV and with a beam current of 20 nA. The beam diameter was ca. 1 μm. The following standards were used for quantitative elemental analyses: zircon (Zr, Si), Hf metal (Hf), UO₂ (U), ThO₂ (Th), apatite (P), YPO₄ (Y), topaz (Al), hornblende (Fe, Ca), and Pb-rich glass (Pb). Peaks and backgrounds for most elements were measured with counting times of 20 and 10 s, respectively, apart from Si (10 s on peak; 5 s on background). All data were reduced using the ZAF correction program.

RESULTS

Minerals of the zircon–hafnon series were found in the contact zone, Zone I, Zone II, and Zone III, although they are most common in Zone III (cleavelandite–quartz–spodumene zone). In total, 160 EPMA spot measurements were performed on 68 zircon–hafnon grains from these textural zones.

Zircon in the contact zone

Five irregularly shaped zircon grains were observed in one thin-section from the contact zone. These zircons are subhedral to anhedral and 20–80 μm in size (Fig. 3). Associated minerals are schorl, dravite, muscovite, apatite, and manganocolumbite (Fig. 3a). The zircon grains have a porous appearance, which might be related to metamictization after crystallization. Some zircon

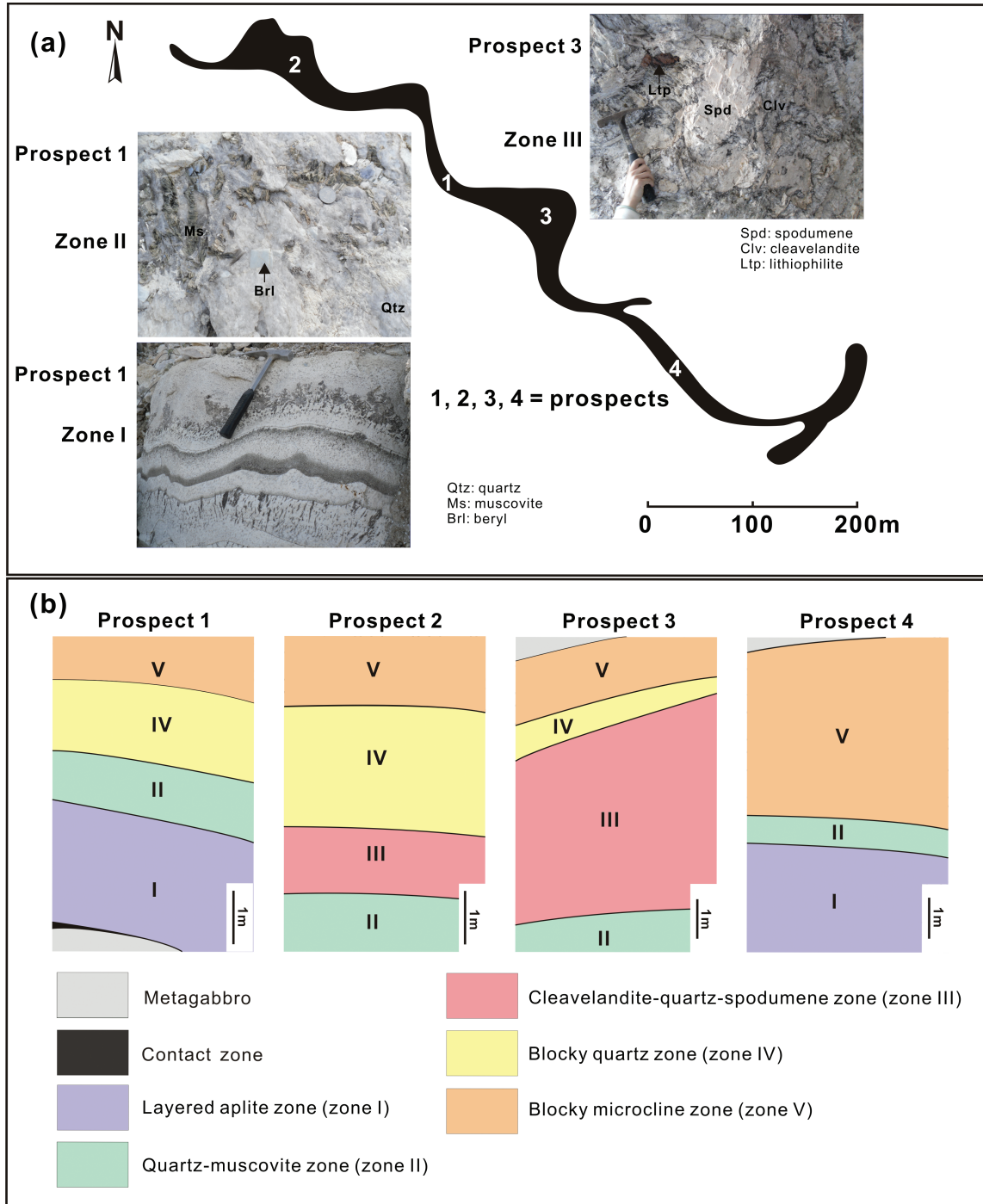


FIGURE 2. (a) Schematic map of the Koktokay No. 1 pegmatite and locations of the observed prospects. (b) Schematic sections of the textural zonation in the Koktokay No. 1 pegmatite at four prospects.

grains also contain quartz and thorite inclusions ($<5\ \mu\text{m}$ in size). The zircon grain shown in Figure 3b appears to be an aggregate of smaller zircon grains, which exhibits variable Z-contrast in the BSE image, with darker cores surrounded by brighter rims.

Four zircon grains in this zone with porous (and metamict) features have variably low oxide totals. HfO_2 contents are

relatively low and range from 3.58 to 6.17 wt% (Hf no. = 0.03–0.06; Table 1), leading to a classification of zircon in the zircon–hafnon series (Fig. 4). The zircon grain shown in Figure 3b has relatively high and variable HfO_2 contents. The dark cores contain 6.68–9.38 wt% HfO_2 (Hf no. = 0.06–0.09), whereas the bright rims contain 18.01–18.68 wt% HfO_2 (Hf no. = 0.17–0.18).

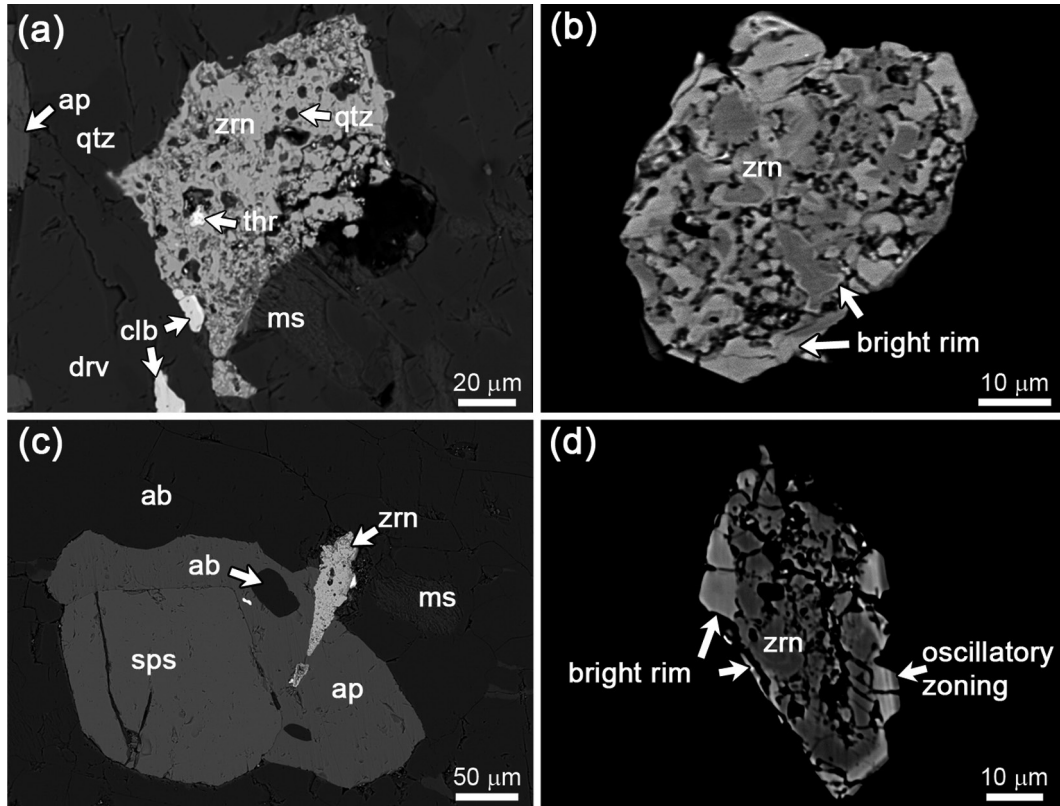


FIGURE 3. Backscattered electron images of zircon from the contact (a–b) and aplite zone (c–d). Abbreviations: zrn = zircon, ms = muscovite, drv = dravite, ap = apatite, sps = spessartine, tht = thorite, clb = columbite, ab = albite.

TABLE 1. Representative EMPA compositions of zircon from the contact zone, Zone I, and Zone II of the Kottokay No. 1 pegmatite*

	Contact zone				Zone I			Zone II and its muscovite aggregates					
	n	m	b	n	m	b	n	m	s	n	r	m	
SiO ₂	30.81	32.54	27.55	31.06	32.34	21.99	32.34	33.18	22.55	32.50	31.30	30.10	22.28
ZrO ₂	64.62	58.18	64.31	50.07	57.69	44.75	55.08	54.73	54.38	59.43	56.76	36.72	28.45
HfO ₂	4.20	9.38	3.92	18.48	9.63	4.24	13.03	11.46	4.44	7.51	11.45	33.80	31.30
UO ₂	0.11	–	0.27	–	0.36	1.05	0.09	0.04	0.16	0.25	–	0.14	0.31
ThO ₂	–	–	0.27	–	–	2.53	–	–	–	–	–	0.07	0.14
P ₂ O ₅	–	–	0.08	–	0.22	5.35	–	–	–	–	–	–	–
Y ₂ O ₃	0.08	0.04	0.13	–	–	0.19	–	–	–	–	–	–	0.08
Al ₂ O ₃	0.03	–	0.12	–	0.15	1.89	–	–	2.82	0.03	–	–	0.62
FeO	0.18	–	0.84	–	0.00	2.29	0.08	–	0.07	0.02	–	–	0.12
CaO	0.13	–	0.38	–	0.32	3.89	–	–	5.38	–	–	–	3.65
Total	100.2	100.1	97.87	99.61	100.7	88.17	100.6	99.41	89.8	99.74	99.51	100.8	86.95
Calculated based on 4 O atoms													
Si	0.966	1.023	0.904	1.022	1.013	0.782	1.027	1.051	0.809	1.020	1.004	1.044	0.933
Zr	0.989	0.892	1.029	0.804	0.882	0.776	0.853	0.845	0.951	0.910	0.888	0.621	0.581
Hf	0.037	0.084	0.037	0.173	0.086	0.043	0.118	0.103	0.045	0.067	0.104	0.333	0.373
U	0.001	–	0.002	–	0.003	0.008	0.001	–	0.001	0.002	–	0.001	0.003
Th	–	–	0.002	–	–	0.020	–	–	–	–	–	0.001	0.001
P	–	–	0.002	–	0.006	0.161	–	–	–	–	–	–	–
Y	0.001	0.001	0.002	–	–	0.004	–	–	–	–	–	–	0.002
Al	0.001	–	0.005	–	0.006	0.079	–	–	0.119	0.001	–	–	0.031
Fe	0.005	–	0.023	–	–	0.068	0.002	–	0.002	0.001	–	–	0.004
Ca	0.004	–	0.013	–	0.011	0.148	–	–	0.207	–	–	–	0.164
Hf no.	0.04	0.09	0.03	0.18	0.09	0.15	0.12	0.11	0.05	0.07	0.11	0.35	0.39

Notes: * Pb contents were also measured but are not shown because they were below or close to the detection limit; n = normal zircon with ~100 wt% oxide totals; m = zircon with metamict texture; b = bright zircon rim; s = secondary zircon shown in Figure 5a; r = relict zircon shown in Figure 5f. Dash (–) denotes below the detection limit. Hf no. = molar Hf/(Zr + Hf).

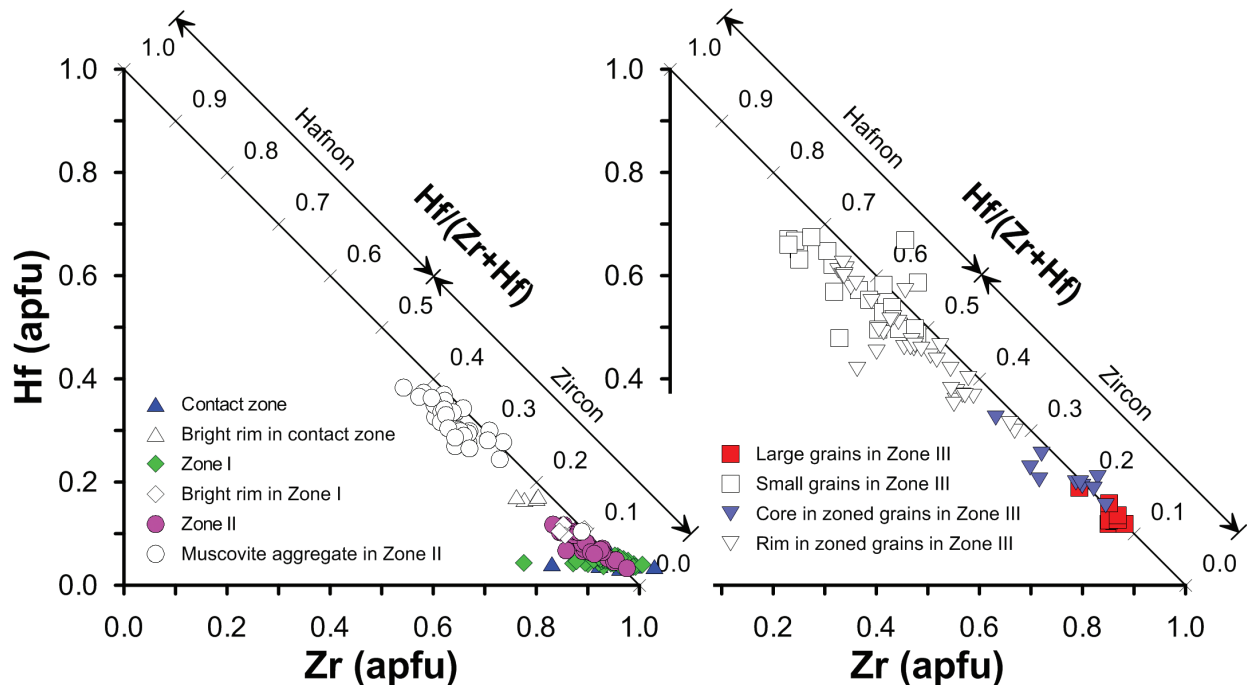


FIGURE 4. Plots of Zr vs. Hf (apfu) in zircon from different zones.

Zircons contain low contents of ThO_2 and UO_2 (average 0.05 and 0.06 wt%, respectively).

Zircon in the aplite zone (Zone I)

Twenty-two zircon grains from seven polished thin-sections were analyzed from Zone I. Zircon grains in this zone have a close association with apatite (Fig. 3c) and are also interstitial to rock-forming minerals such as albite and quartz. The zircons are subhedral to anhedral in shape and most are $<100\ \mu\text{m}$ in size. Some quartz inclusions that are $<3\ \mu\text{m}$ in size are present in the zircon grains, along with some micrometer-sized thorite inclusions. Zircon grains in Zone I have two main characteristics: (1) most grains are porous and may have experienced metamictization; and (2) some zircon grains have a thin bright rim and, in one grain, the bright rim exhibits oscillatory zoning (Fig. 3d).

Zircon grains in Zone I have variable oxide totals (from 88.17 to ~ 100 wt%) and contain 3.51–9.63 wt% HfO_2 (Hf no. = 0.03–0.09) (Table 1; Fig. 4), corresponding to zircon in the zircon–hafnon solid-solution series. However, the bright rims identified in BSE images typically have normal oxide totals (~ 100 wt%) and contain 10.75–13.03 wt% HfO_2 (Hf no. = 0.10–0.12) and are hafnian zircon. The zircon grains with low oxide totals in Zone I usually have high contents of ThO_2 (up to 2.53 wt%), UO_2 (up to 1.05 wt%), CaO (up to 4.23 wt%), FeO (up to 3.72 wt%), Al_2O_3 (up to 2.14 wt%), and P_2O_5 (up to 5.35 wt%).

Zircon in the quartz–muscovite zone (Zone II)

Zircon grains in Zone II are subhedral to anhedral and are relatively large (70–300 μm). These zircons mainly occur interstitially between rock-forming minerals. All zircon grains in this zone exhibit complex internal textures (Fig. 5). The zircon

grain shown in Figure 5a has a euhedral core surrounded by a fine-grained anhedral rim. Some regions between the core and rim are metamict. One grain has oscillatory zoning but exhibits a general trend of becoming brighter from core to rim (Fig. 5b). Two large zircon grains were observed in nest-like muscovite aggregates (Figs. 5c–5f). One of these shows both metamictization and patchy zoning (Figs. 5c–5d). The other has experienced strong metamictization and contains a few irregular relict regions (Figs. 5e–5f). Some of these relict regions are connected with a bright zone at the margin (e.g., Fig. 5f).

Most zircon grains in Zone II contain 3.26–13.04 wt% HfO_2 (Hf no. = 0.03–0.12) and are zircon to hafnian zircon (Fig. 4). Different regions of the grain shown in Figure 5a have variable HfO_2 contents. The euhedral core has a normal oxide total (~ 100 wt%) and contains 11.46 wt% HfO_2 (Hf no. = 0.11). The metamict regions in this grain have low oxide totals of ca. 90 wt%, contain several wt% of Al_2O_3 and CaO, and have HfO_2 contents of 4.44–5.16 wt% (Hf no. = 0.05) (Table 1). The fine-grained zircon in the anhedral rim has normal oxide totals and has higher HfO_2 (7.46–7.90 wt%) than the metamict zircon regions. The Hf no. value of the fine-grained zircon is 0.07. Unlike most zircon grains in Zone II, the two zircon grains observed in the nest-like muscovite aggregates contain much higher HfO_2 (11.45–36.06 wt%), and some analyses have >25 wt% HfO_2 with Hf no. values ranging from 0.25 to 0.41 (Fig. 4). Although the metamict regions in the grains shown in Figures 5c–5f have low oxide totals (80.1–90.7 wt%), they have HfO_2 contents (25.10–31.30 wt%) similar to, and SiO_2 (19.23–26.09 wt%) and ZrO_2 (25.70–34.83 wt%) contents lower than, those of the intact zircon regions (including the relict regions in Fig. 5f) (Table 1). The metamict zircon regions also have high CaO (up to 5.38 wt%) and Al_2O_3 (up to 2.82 wt%).

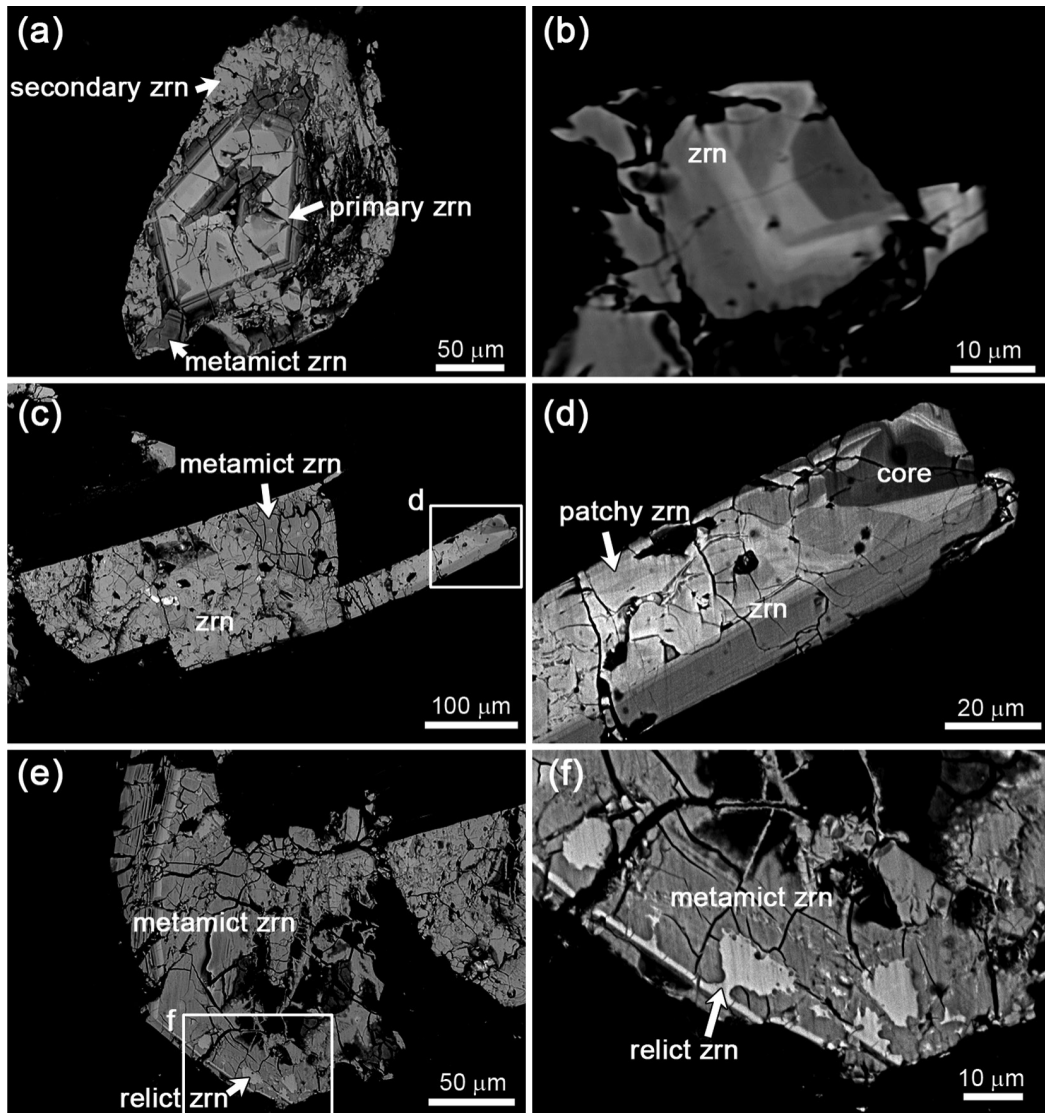


FIGURE 5. Backscattered electron images of zircon grains from the quartz–muscovite zone (a–b) and the nest-like muscovite aggregates (c–f). As in Figure 3, zrn = zircon.

Zircon (*sl*) in the cleavelandite–quartz–spodumene zone (Zone III)

Zircon (*sl*) grains are common in Zone III (36 grains in three thin-sections) and exhibit variable petrographic features. Some zircon grains ($n = 12$) are interstitial to or included within albite (Fig. 6a). Most of the zircons are large (up to 500 μm) and contain small quartz inclusions (<1 μm in size) (Fig. 6b). The latter feature is similar to that of typical magmatic zircon from the contact and aplite zones. There are no large chemical variations within these single zircon grains, but some variation was observed between different grains (Table 2). HfO_2 contents vary from 12.99 to 19.45 wt% (Hf no. = 0.12–0.19; “Large grains” in Fig. 4b), leading to a classification of hafnian zircon.

Other zircon grains in Zone III appear to be closely associated with muscovite and/or spodumene (Fig. 7), although some of these zircons are also associated with albite. The muscovite associated with zircon in this zone is small (e.g., Fig. 7a) and

is either intergrown with albite or occurs interstitially to large spodumene or manganotantalite grains (e.g., Fig. 7f). These zircon grains are <100 μm in size and most are <20 μm in size. Unlike the typical magmatic zircon in this zone (Fig. 6), no quartz inclusions were observed within these zircon grains. Most of the zircon grains associated with muscovite and spodumene exhibit chemical zoning or contain patchy, bright alteration regions in BSE images (Figs. 7c–7f). EPMA results revealed that these zircon grains are strongly Hf-enriched and have a large range of HfO_2 contents from 16.30 to 58.88 wt% (Hf no. = 0.15–0.75; Fig. 4b), even within single crystals (Table 2). Small unzoned zircon grains (“Small grains” in Fig. 4b) are markedly Hf-enriched with Hf no. values ranging from 0.50 to 0.75, leading to a classification of zirconian hafnon. Within zoned zircon grains, the cores usually have lower HfO_2 contents (16.30–32.26 wt%) than the rims (29.91–56.08 wt%), and the patchy, bright alteration regions typically have HfO_2 contents comparable to the Hf-rich rims. The

FIGURE 6. Backscattered electron images of zircon closely associated with albite in Zone III. These zircon grains are typically large and subhedral to euhedral.

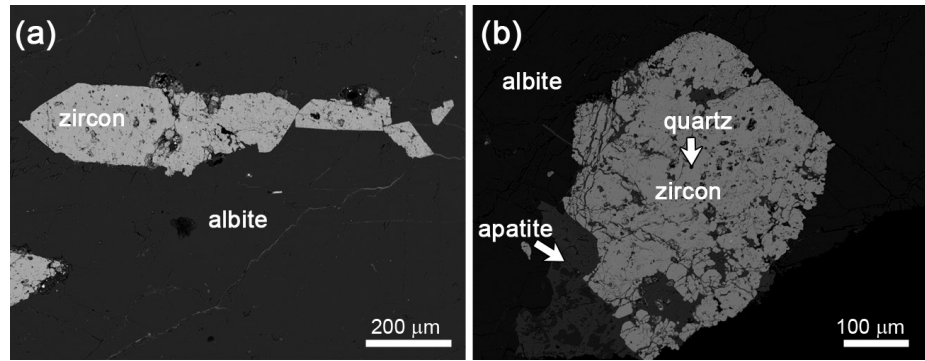


TABLE 2. Representative EMPA compositions of zircon and hafnon from Zone III of the Koptokay No. 1 granitic pegmatite*

	Associated with albite			Associated with muscovite and spodumene										
				Discrete grains			Fig. 7c		Fig. 7d		Fig. 7e		Fig. 7f	
SiO ₂	31.41	29.44	30.88	27.38	25.69	31.13	30.92	28.35	29.47	26.73	30.11	24.68	32.39	27.7
ZrO ₂	54.04	52.20	53.71	11.73	13.88	32.69	49.22	25.78	36.65	17.67	52.1	23.81	44.31	23.04
HfO ₂	13.66	16.66	13.80	58.88	58.59	36.38	21.34	44.76	32.26	56.49	16.3	51.10	21.67	47.63
UO ₂	0.19	0.14	0.14	—	—	0.58	—	0.04	0.08	0.05	0.03	0.09	—	0.28
Al ₂ O ₃	—	—	—	—	0.07	—	—	—	—	—	—	—	0.13	—
FeO	0.05	—	—	0.04	0.19	—	0.02	—	—	—	—	—	—	0.06
CaO	0.02	0.08	0.08	0.03	—	0.02	—	0.03	—	—	0.02	0.03	—	0.10
PbO	0.07	—	0.35	—	—	—	0.02	0.11	—	—	—	0.24	0.53	—
Total	99.44	98.52	98.96	98.06	98.42	100.8	101.5	99.07	98.46	100.94	98.56	99.95	99.03	98.81
Calculated based on four O atoms														
Si	1.018	0.985	1.010	1.098	1.041	1.081	1.014	1.056	1.042	1.04	1.001	0.969	1.073	1.052
Zr	0.854	0.852	0.857	0.229	0.274	0.554	0.787	0.468	0.632	0.335	0.845	0.456	0.716	0.427
Hf	0.126	0.159	0.128	0.671	0.675	0.359	0.199	0.474	0.324	0.625	0.154	0.571	0.204	0.514
U	0.001	0.001	0.001	—	—	0.004	—	—	0.001	—	—	0.001	—	0.002
Al	—	—	—	—	0.003	—	—	—	—	—	—	—	0.005	—
Fe	0.001	—	—	0.001	0.006	—	0.001	—	—	—	—	0.001	—	0.002
Ca	0.001	0.003	0.003	0.001	—	0.001	—	0.001	—	—	0.001	0.001	—	0.004
Pb	0.001	—	0.003	—	—	—	—	0.001	—	—	—	0.003	0.005	0
Hf no.	0.13	0.16	0.13	0.75	0.71	0.39	0.20	0.50	0.34	0.65	0.15	0.56	0.22	0.55

Notes: * P, Th, and Y contents were measured but are not shown because they were below or close to the detection limits. Dash (—) denotes below the detection limit. Hf no. = molar Hf/(Zr + Hf).

largest variation of HfO₂ contents within a single grain is up to ~35 wt% (Hf no. = 0.15–0.56). Two other grains also show large internal HfO₂ variations of up to 25 wt% (Hf no. = 0.34–0.65 and 0.22–0.55). It should be noted that most analyses on zircon (s/l) grains associated with muscovite and spodumene have Hf no. > 0.5, showing that they are zirconian hafnon (Fig. 4b).

To better understand the large Zr–Hf fractionation in other minerals in this zone, we measured ZrO₂ and HfO₂ contents in a large manganotantalite aggregate that was ~5.6 mm in size and closely associated with small zircon grains (e.g., Fig. 7f). The small zircon grains are mainly included in muscovite, which occurs as an interstitial phase between manganotantalite grains or surrounding the manganotantalite aggregate. The manganotantalite aggregate contains Nb-poor and Nb-rich regions. Representative EPMA compositions of the manganotantalite are given in Table 3. The Nb-poor regions have a very high molar Ta/[Nb + Ta] value (0.96–0.97) and contain a few wt% of ZrO₂ (1.5–2.0 wt%) and HfO₂ (0.5–0.8 wt%) with molar Zr/Hf > 3. However, ZrO₂ and HfO₂ contents in the Nb-rich regions (Ta/[Nb + Ta] = 0.52–0.57) within this manganotantalite aggregate are below or close to detection limits (Table 3).

TABLE 3. Representative EPMA compositions of manganotantalite associated with tiny zircon grains in Zone III

	— Nb-poor manganotantalite —				— Nb-rich manganotantalite —	
Ta ₂ O ₅	79.67	80.01	81.20	80.69	53.84	50.41
Nb ₂ O ₅	2.02	1.76	1.97	1.67	27.78	27.88
FeO	0.20	0.27	0.13	0.26	1.49	1.73
MnO	14.80	14.50	14.42	14.52	15.78	15.99
ZrO ₂	1.49	1.92	1.64	1.87	—	—
HfO ₂	0.82	0.67	0.63	0.56	—	0.09
Total	99.00	99.13	99.99	99.57	98.89	96.10
Calculated based on six O atoms						
Ta	1.830	1.836	1.848	1.844	1.064	1.018
Nb	0.077	0.067	0.075	0.063	0.912	0.936
Fe	0.014	0.019	0.009	0.018	0.090	0.107
Mn	1.058	1.035	1.022	1.033	0.970	1.005
Zr	0.061	0.079	0.067	0.077	—	—
Hf	0.019	0.015	0.014	0.013	—	0.002
Ta/(Nb+Ta)	0.96	0.96	0.96	0.97	0.54	0.52
Zr/Hf	3.3	5.1	4.7	6.0	0.0	0.0

Note: Dash (—) denotes below the detection limit.

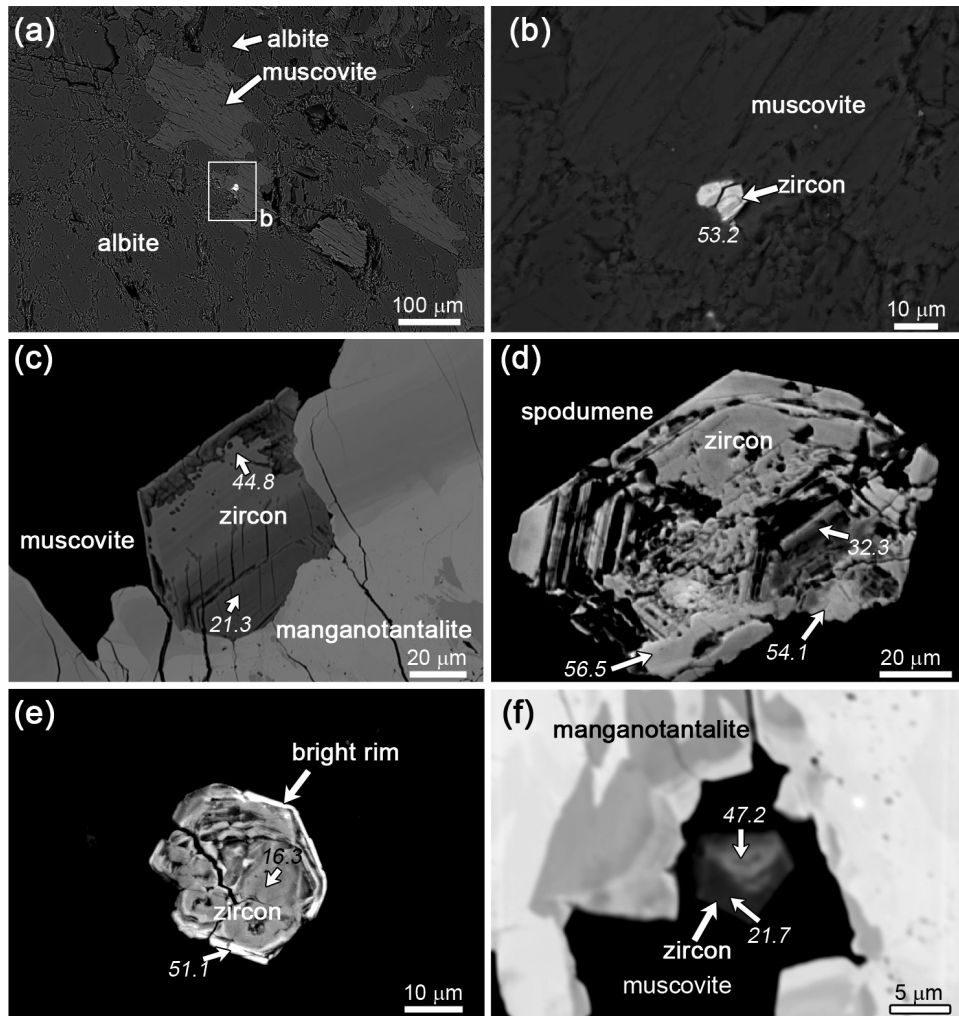


FIGURE 7. Backscattered electron images of zircon (*sl*) associated with muscovite and spodumene in the cleavelandite-quartz-spodumene zone. The italic numbers on the images denote HfO₂ contents (in wt%).

DISCUSSION

Zircon is the major carrier of Zr and Hf in rare-element-bearing granites and pegmatites. Its Hf concentrations may reflect Zr/Hf fractionation in granitic magma, which follows a fractionation trend as is evident from a Hf vs. Zr/Hf plot for zircon (Černý et al. 1985). Zircon from granites usually contains 1–3 wt% HfO₂, whereas zircon from rare-element-bearing granites and pegmatites may be more strongly enriched in Hf (Černý et al. 1985). Examples of Hf-rich zircon have been described in the Tanco granitic pegmatite (Černý and Siivola 1980; Van Lichtervelde et al. 2009) and in granitic pegmatites from the central-western Carpathians, Slovakia (Uher and Černý 1998). The highest HfO₂ value measured to date in zircon is ca. 35 wt% (Suzhou rare-element-bearing granite; Wang et al. 1996; Koptokay No. 3 pegmatite; Zhang et al. 2004b). The Hf-dominant end-member of the zircon-hafnon solid solution has only been described from its type locality in Zambézia in 1974 (Correia Neves et al. 1974).

In the Koptokay No. 1 pegmatite, zircon exhibits large chemical variations, not only between different zones, but also within single pegmatite zones, and even in single crystals (Figs. 4 and

8). EPMA results reveal that many grains in Zone III are strongly Hf-enriched and are zirconian hafnon with Hf no. values up to 0.75. This is the first report of zirconian hafnon in natural samples since the discovery of hafnon 40 years ago (Correia Neves et al. 1974). The presence of abundant zirconian hafnon indicates that the Koptokay No. 1 pegmatite is a highly evolved granitic pegmatite. It also provides an important and unique opportunity to constrain the evolution from zircon to hafnon.

In subsequent sections, we discuss the possible cause(s) of the evolution from zircon to hafnon in the Koptokay No. 1 pegmatite, based mainly on published experimental results (e.g., Ellison and Hess 1986; Keppler 1993; Linnen 1998; Linnen and Keppler 2002; Linnen and Cuney 2005) and observations from the present study. The fractionation trend of Zr/Hf in zircon-hafnon is conventionally explained on the basis of differential solubilities of the two end-member phases in metaluminous to peraluminous granitic melts (Linnen and Cuney 2005). Previous experimental studies have considered factors that might affect the solubilities of zircon and hafnon in melts (e.g., Ellison and Hess 1986; Linnen 1998; Linnen and Keppler 2002), which include fractional

crystallization of granitic magma (changing melt composition and temperature), buffering effects of other Zr-bearing phases, and the role of fluxes such as Li and F.

The solubilities of zircon and hafnon in silicate melts of various granitic compositions have been experimentally studied (e.g., Ellison and Hess 1986; Keppler 1993; Linnen 1998; Linnen and Keppler 2002). All of these studies have shown that solubilities of both zircon and hafnon decrease with increasing alumina saturation indices (e.g., molar $\text{Al}/[\text{Na} + \text{K}]$ ratio; ASI) of anhydrous and hydrous melts. Li is also an alkali element; however, apart from Zone III, no Li-rich minerals were observed in the Koktokay No. 1 pegmatite. Thus, we do not include Li in the ASI when considering the Zr/Hf fractionation in different textural zones. The experimental results of Linnen and Keppler (2002) indicate that ASI might significantly affect Zr/Hf ratios in aluminous melts ($\text{ASI} > 0.9$). Magmatic crystallization would decrease the Zr/Hf value in late-stage magmas and result in Hf enrichment in late-crystallizing zircon. Similarly, the experiments of Linnen and Keppler (2002) showed that lower temperatures could result in large Zr/Hf fractionations in granitic melts, particularly in peraluminous granitic magma. Therefore, crystallization of zircon in peraluminous granitic melt at relatively low temperatures would result in a progressive fractionation of Zr from Hf. The Koktokay No. 1 pegmatite is peraluminous, as is evident from the presence of abundant Al-rich minerals. In addition, Wu (1994) measured the formation temperatures of fluid inclusions in spodumene from Zone III of the Koktokay No. 1 pegmatite. These temperatures

were ca. 350 °C, which are much lower than the temperatures under which most of the experimental studies were conducted (Linnen and Keppler 2002). Thus, it can be inferred that zircon in the Koktokay No. 1 pegmatite would exhibit a high degree of Zr/Hf fractionation. In fact, the gradual increase of Hf no. values of typical magmatic zircon grains (Fig. 8a) from the contact zone (0.03–0.09), through Zone I (0.03–0.09) and Zone II (0.05–0.12), and to Zone III (0.12–0.19; large zircon grains) is probably the result of fractional crystallization of pegmatitic magma. However, a clear gap in Hf no. values exists between the two separate populations of large and small zircon grains in Zone III (Fig. 8). This abrupt change in Hf concentrations cannot solely be explained by fractional crystallization of pegmatitic magma (Zhang et al. 2004; Van Lichtervelde et al. 2009) and, as such, probably requires the influence of other factors.

Although zircon is the main carrier of Zr and Hf in granitic pegmatites, it is possible that crystallization of other Zr–Hf-bearing minerals (e.g., garnet and columbite-group minerals) can cause Zr/Hf fractionation in residual melts that is then captured by late-crystallizing zircon grains (e.g., Linnen and Keppler 2002). Linnen and Keppler (2002) compiled Zr and Hf solubility data for garnet from the literature (Fujinawa and Green 1997; Green et al. 2000; Van Westrenen et al. 1999, 2000). These data indicate that Zr is preferentially incorporated with respect to Hf in garnet. This implies that garnet crystallization would cause enrichment of Hf relative to Zr in residual melts. However, garnet is scarce in all textural zones of the Koktokay

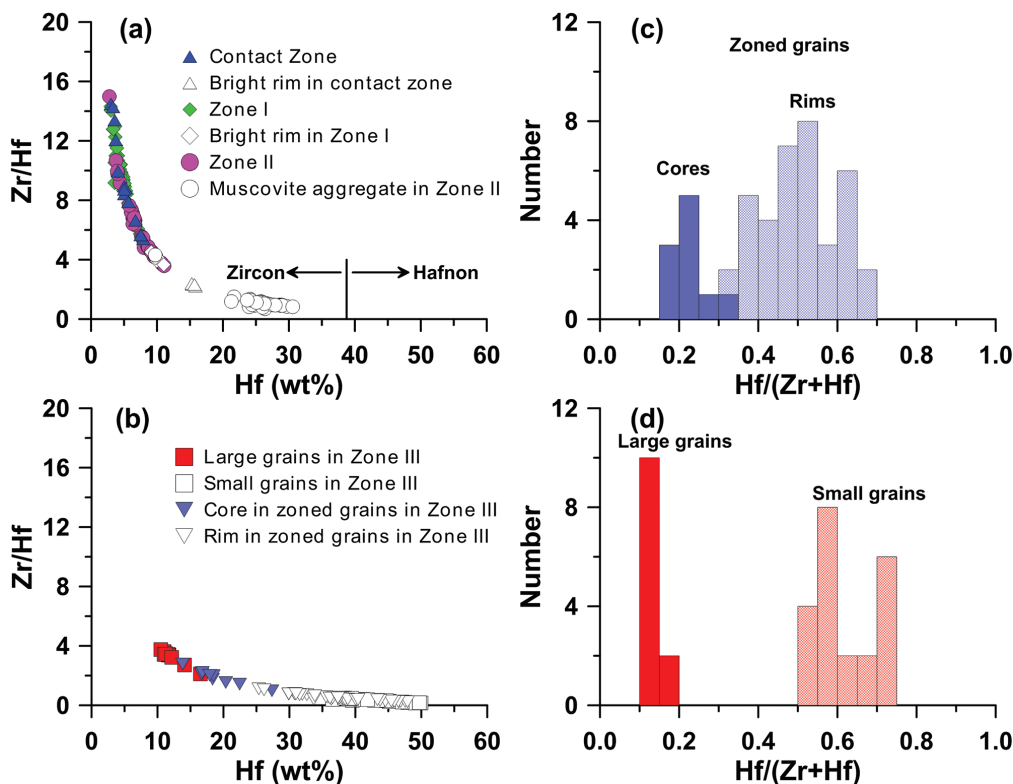


FIGURE 8. (a and b) Zr/Hf fractionation trend for all types of zircon (*sl*) in the Koktokay No. 1 pegmatite. (c and d) Histograms of the Hf/[Zr + Hf] ratio in zircon (*sl*) from Zone III.

No. 1 pegmatite, and thus is unlikely to have been responsible for driving Zr/Hf fractionation in zircons from this pegmatite. Nb-Ta oxides are commonly associated with zircon in rare metal granites and granitic pegmatites (e.g., Wang et al. 1996; Zhang et al. 2004b; Van Lichtervelde et al. 2009). Moreover, Van Lichtervelde et al. (2009) found that zircon can contain a few wt% of Ta₂O₅. In our study, we measured ZrO₂ and HfO₂ contents in manganotantalite closely associated with zircon. The Nb-rich regions contain very low ZrO₂ and HfO₂, whereas Nb-poor manganotantalite (Ta/[Nb + Ta] = ~0.96–0.97) may contain ca. 3 wt% of ZrO₂ and HfO₂. These data demonstrate that crystallization of Nb-rich manganotantalite (and columbite) will not cause Zr/Hf fractionation in granitic melts. Therefore, crystallization of Nb-poor manganotantalite could cause a decrease in Zr/Hf values in granitic melt because of its high Zr/Hf values (>3). However, apart from Zone III, Nb-rich manganotantalite is the dominant Nb-Ta oxide in the Koktokay No. 1 pegmatite, meaning that its crystallization cannot have significantly contributed to the Zr/Hf fractionation in zircon from the contact zone through to the center of the pegmatite.

As discussed above, the sudden Hf-enrichment as marked by the appearance of zirconian hafnon (Figs. 4 and 8) cannot be accounted for by magmatic fractional crystallization. As such, it is necessary to consider the role of fluxes. Commonly cited fluxing components in pegmatite magmas are H₂O, B, F, and P (London 1997). Highly fluxed melts can be the transport medium for incompatible elements, including Zr and Hf. Experiments by Keppler (1993) showed a positive dependence of zircon solubility on F content in peraluminous melts. Similar results have documented the important influence of F on the solubility of zircon and hafnon in granitic magma (Aseri 2012). In contrast, the solubilities of both zircon and hafnon decrease with increasing Li (Linnen 1998), which probably relates to competition between Zr-Hf and Li for binding with a non-bridging oxygen atom.

Zirconian hafnon in the Koktokay No. 1 pegmatite is only present in Zone III and is closely associated with muscovite and spodumene (Fig. 7). It should be noted that Li-rich minerals such as spodumene, lepidolite, and lithiophilite mainly occur in this zone. As such, Li-F coupled fluxing effects may explain the extreme Zr/Hf fractionation of zircon during pegmatite evolution of this zone. Hafnon is observed as crystals interstitial to spodumene (Fig. 7d), indicating that hafnon crystallization took place after spodumene. Crystallization of spodumene may have decreased Li in the residual melt, which in turn enhanced the solubilities of zircon and hafnon. Fluorine also becomes more abundant during the evolution of the Koktokay No. 1 pegmatite. In Zone III, F-bearing minerals are common and include muscovite, tourmaline, lithiophilite, and apatite. High F contents may have effectively increased the solubility of Zr and Hf by forming Zr-Hf-bearing fluoro-complexes (e.g., K₂[Zr,Hf]F₆; Keppler 1993; Niu 2011; Aseri 2012). However, K₂ZrF₆ has a lower solubility than K₂HfF₆ in water-rich fluid (Niu 2011), and this could have enhanced the Zr/Hf fractionation. Therefore, crystallization of spodumene coupled with the effect of fluxing elements like F and Li may have caused the large Zr/Hf fractionation and triggered hafnon crystallization.

In summary, we report the occurrence of rare zirconian hafnon in the Koktokay No. 1 pegmatite from northwestern

China. Fractional crystallization of pegmatitic magma played an important role in driving the margin-to-core Zr/Hf fractionation in these highly evolved granitic pegmatites. However, the extreme evolution from zircon to hafnon is apparently related to high flux components (e.g., Li-F) during the late stages of pegmatite evolution.

ACKNOWLEDGMENTS

The authors thank Wen-Lan Zhang, Xiao-Ming Chen, and Bin Wu for their assistance with EPMA measurements, and Lei Xie for help during fieldwork. Critical comments by M. Van Lichtervelde and T.S. Ercit helped to improve an early version of the manuscript. This work was financially supported by the Natural Science Foundation of China (Grant No. 41230315).

REFERENCES CITED

- Aseri, A. (2012) Effects of fluorine on the solubilities of Nb, Ta, Zr and Hf minerals in highly fluxed water-saturated haplogranitic melts, pp. 74. Master thesis, University of Waterloo, Ontario.
- Belousova, E.A., Griffin, W.L., O'Reilly, S.Y., and Fisher, N.I. (2002) Igneous zircon: trace element composition as an indicator of source rock type. *Contributions to Mineralogy and Petrology*, 143, 602–622.
- Černý, P., and Siivola, J. (1980) The Tanco pegmatite at Bernic Lake, Manitoba XII. hafnian zircon. *Canadian Mineralogist*, 18, 313–321.
- Černý, P., Meintzer, R.E., and Anderson, A.J. (1985) Extreme fractionation in rare-element granitic pegmatites: selected examples of data and mechanisms. *Canadian Mineralogist*, 23, 381–421.
- Correia Neves, J.M., Lopes Nunes, J.E., and Sahama, T.G. (1974) High hafnium members of the zircon-hafnon series from the granite pegmatites of Zambézia, Mozambique. *Contributions to Mineralogy and Petrology*, 48, 73–80.
- Ellison, A.J., and Hess, P.C. (1986) Solution behavior of +4 cations in high silica melts: petrologic and geochemical implications. *Contributions to Mineralogy and Petrology*, 94, 343–351.
- Fujinawa, A., and Green, T.H. (1997) Partitioning behaviour of Hf and Zr between amphibole, clinopyroxene, garnet and silicate melts at high pressure. *European Journal of Mineralogy*, 9, 379–391.
- Green, T.H., Blundy, J.D., Adam, J., and Yaxley, G.M. (2000) SIMS determination of trace element partition coefficients between garnet, clinopyroxene and hydrous basaltic liquids at 2–7.5 GPa and 1080–1200 °C. *Lithos*, 53, 165–187.
- Keppler, P. (1993) Influence of fluorine on the enrichment of high field strength trace elements in granitic rocks. *Contributions to Mineralogy and Petrology*, 114, 479–488.
- Linnen, R.L. (1998) The solubility of Nb-Ta-Zr-Hf-W in granitic melts with Li and Li+F: constrains for mineralization in rare metal granites and pegmatites. *Economic Geology*, 93, 1013–1025.
- Linnen, R.L., and Cuney, M. (2005) Granite-related rare-element deposits and experimental constraints on Ta-Nb-W-Sn-Zr-Hf mineralization. In R.L. Linnen and I.M. Samson, Eds., *Rare-Element Geochemistry and Mineral Deposits*, 17, p. 70–102. Geological Association of Canada Short Course Notes, St. John's, Newfoundland, Canada.
- Linnen, R.L., and Keppler, H. (2002) Melt composition control of Zr-Hf fractionation in magmatic processes. *Geochimica et Cosmochimica Acta*, 66, 3293–3301.
- London, D. (1997) Estimating abundances of volatile and other mobile components in evolved silicic melts through mineral-melt equilibria. *Journal of Petrology*, 38, 1691–1706.
- Ma, C., and Rossman, G.R. (2005) Microanalysis of hafnian zircon. *Microscopy and Microanalysis*, 11, 1304–1305.
- Niu, Y.L. (2011) Earth processes cause Zr-Hf and Nb-Ta fractionations, but why and how? *RSC Advances*, 2, 3587–3591.
- Ramakrishnan, S.S., Gokhale, K.V.G.K., and Subbarao, E.C. (1969) Solid solubility in the system zircon-hafnon. *Materials Research Bulletin*, 4, 323–328.
- Shannon, R.D. (1976) Revised effective ionic radii and systematic studies of interatomic distances in halides and chalcogenides. *Acta Crystallographica*, A32, 751–767.
- Uher, P., and Černý, P. (1998) Zircon in Hercynian granitic pegmatites of the western Carpathians, Slovakia. *Geologica Carpathica Clays*, 49, 261–270.
- Van Lichtervelde, M., Melcher, F., and Wirth, R. (2009) Magmatic vs. hydrothermal origins for zircon associated with tantalum mineralization in the Tanco pegmatite, Manitoba, Canada. *American Mineralogist*, 94, 439–450.
- Van Lichtervelde, M., Holtz, F., and Hancher, J.M. (2010) Solubility of manganotantalite, zircon and hafnon in highly fluxed peralkaline to peraluminous pegmatitic melts. *Contributions to Mineralogy and Petrology*, 160, 17–32.
- Van Westrenen, W., Blundy, J., and Wood, B. (1999) Crystal-chemical controls on trace element partitioning between garnet and anhydrous silicate melt. *American Mineralogist*, 84, 838–847.
- Van Westrenen, W., Blundy, J.D., and Wood, B.J. (2000) Effect of Fe²⁺ on garnet-

- melt trace element partitioning: Experiments in FCMAS and quantification of crystal-chemical controls in natural systems. *Lithos*, 53, 189–201.
- Wang, X.J., Zou, T.R., Xu, J.G., Yu, X.Y., and Qiu, Y.Z. (1981) Study of pegmatite minerals of the Altai region, pp. 156. Science Publishing House, Beijing (in Chinese).
- Wang, R.C., Fontan, F., Xu, S.J., Chen, X.M., and Monchoux, P. (1996) Hafnian zircon from the apical part of the Suzhou granite, China. *Canadian Mineralogist*, 34, 1001–1010.
- Wang, R.C., Hu, H., Zhang, A.C., Fontan, F., Zhang, H., and de Parseval, Ph. (2006) Occurrence and late re-equilibration of pollucite from the Koktokay no. 3 pegmatite, Altai, northwestern China. *American Mineralogist*, 91, 729–739.
- Wang, R.C., Hu, H., Zhang, A.C., Fontan, F., de Parseval, Ph., and Jiang, S.Y. (2007a) Cs-dominant polyolithionite in the Koktokay#3 pegmatite, Altai, NW China: in situ micro-characterization and implication for the storage of radioactive cesium. *Contributions to Mineralogy and Petrology*, 153, 355–367.
- Wang, T., Tong, Y., Jahn, B.M., Zou, T.R., Wang, Y.B., Hong, D.W., and Han, B.F. (2007b) SHRIMP U–Pb Zircon geochronology of the Altai No. 3 Pegmatite, NW China, and its implications for the origin and tectonic setting of the pegmatite. *Ore Geology Reviews*, 32, 325–336.
- Wang, R.C., Che, X.D., Zhang, W.L., Zhang, A.C., and Zhang, H. (2009) Geochemical evolution and late re-equilibration of Na-Cs-rich beryl from the Koktokay no.3 pegmatite (Altai, NW China). *European Journal of Mineralogy*, 21, 795–809.
- Windley, B.F., Kroener, A., Guo, J., Qu, G., Li, Y., and Zhang, C. (2002) Neoproterozoic to Paleozoic geology of the Altai Orogen, NW China: new zircon age data and tectonic evolution. *Journal of Geology*, 110, 719–737.
- Wu, B.Q., and Zou, T.R. (1989) The genesis of granitic pegmatites in Xinjiang Altai. *Mineral and Geology of Xinjiang*, 1, 60–70 (in Chinese).
- Wu, C.N. (1994) Geochemical evolution and mineralization of No. 3 pegmatite vein in Keketuohai, Xinjiang. Ph.D. thesis, pp. 123. Nanjing University, Nanjing.
- Xiao, X.C., Tang, Y.Q., Feng, Y., Zhu, B., Li, J., and Zhou, M. (1992) Tectonics in northern Xinjiang and its neighbouring areas. Geological Publishing, Beijing, p. 104–121 (in Chinese with English abstract).
- Zhang, A.C., Wang, R.C., Hu, H., Chen, X.M., and Zhang, H. (2004a) Occurrences of foitite and rossmanite from the Koktokay No. 3 granitic pegmatite dike, Altai, northwestern China: a record of hydrothermal fluids. *Canadian Mineralogist*, 42, 837–882.
- Zhang, A.C., Wang, R.C., Hu, H., Zhang, H., Zhu, J.C., and Chen, X.M. (2004b) Chemical evolution of Nb-Ta oxides and zircon from the Koktokay No. 3 granitic pegmatite, Altai, northwestern China. *Mineralogical Magazine*, 68, 739–756.
- Zhang, A.C., Wang, R.C., Jiang, S.Y., Hu, H., and Zhang, H. (2008a) Chemical and textural features of tourmaline from the spodumene-subtype Koktokay No. 3 pegmatite, northwestern China: a record of magmatic to hydrothermal evolution. *Canadian Mineralogist*, 46, 41–58.
- Zhang, A.C., Wang, R.C., Li, Y.L., Hu, H., Lu, X.C., Ji, J.F., and Zhang, H. (2008b) Tourmalines from the Koktokay No. 3 pegmatite, Altai, NW China: spectroscopic characterization and relationships with the pegmatite evolution. *European Journal of Mineralogy*, 20, 143–154.

MANUSCRIPT RECEIVED FEBRUARY 4, 2013

MANUSCRIPT ACCEPTED JUNE 15, 2013

MANUSCRIPT HANDLED BY SIMON REDFERN